

RESEARCH

Open Access



Genome-wide DNA methylation analysis reveals a unique methylation pattern for pleural mesothelioma compared to healthy pleura and other lung diseases

Janah Vandenhoeck^{1,2}, Joe Ibrahim^{1,2}, Nele De Meulenaere^{1,2}, Dieter Peeters³, Jo Raskin⁴, Jeroen M. H. Hendriks^{5,6}, Paul Van Schil^{5,6}, Jan van Meerbeeck⁴, Guy Van Camp^{1,2} and Ken Op de Beeck^{1,2*} 

Abstract

Background Pleural mesothelioma (PM) is a rare and aggressive cancer type, typically diagnosed at advanced stages. Distinguishing PM from other lung diseases is often challenging. There is an urgent need for biomarkers that can enable early detection. Interest in the field of epigenetics has increased, particularly in the context of tumour development and biomarker discovery. This study aims to identify specific changes in DNA methylation from healthy pleural tissue to PM and to compare these methylation patterns with those found in other lung diseases.

Results EPIC methylation array data (850 K) were generated for 11 PM and 29 healthy pleura in-house collected samples. This is the first time such a large dataset of healthy pleura samples has been generated. Additional EPIC methylation array data (850 K) for pleural mesothelioma and other lung-related diseases were downloaded from public databases. We conducted pairwise differential methylation analyses across all tissue types, which facilitated the identification of significantly differentially methylated CpG sites. Extensive differential methylation between PM and healthy pleura was observed, identifying 81,968 differentially methylated CpG sites across all genomic regions. Among these, five CpG sites located within four genes (*MIR21*, *RNF39*, *SPEN* and *C1orf101*) exhibited the most significant and pronounced methylation differences between PM and healthy pleura. Moreover, our analysis delineated distinct methylation patterns specific to PM subtypes. Finally, the methylation profiles of PM were distinctly different from those of other lung cancers, enabling accurate differentiation.

Conclusions DNA methylation analyses provide a robust method for distinguishing PM from healthy pleural tissues, and specific methylation patterns exist within PM subtypes. These methylation differences underscore their importance in understanding disease progression and may serve as viable biomarkers or therapeutic targets. Moreover, differential methylation patterns between PM and other lung cancers highlights its diagnostic potential. These findings necessitate further translational studies to explore their clinical applications.

Keywords Epigenetics, DNA methylation, Pleural mesothelioma, Lung cancer, Healthy pleura

*Correspondence:

Ken Op de Beeck

Ken.opdebeeck@uantwerpen.be

Full list of author information is available at the end of the article



© The Author(s) 2024. **Open Access** This article is licensed under a Creative Commons Attribution-NonCommercial-NoDerivatives 4.0 International License, which permits any non-commercial use, sharing, distribution and reproduction in any medium or format, as long as you give appropriate credit to the original author(s) and the source, provide a link to the Creative Commons licence, and indicate if you modified the licensed material. You do not have permission under this licence to share adapted material derived from this article or parts of it. The images or other third party material in this article are included in the article's Creative Commons licence, unless indicated otherwise in a credit line to the material. If material is not included in the article's Creative Commons licence and your intended use is not permitted by statutory regulation or exceeds the permitted use, you will need to obtain permission directly from the copyright holder. To view a copy of this licence, visit <http://creativecommons.org/licenses/by-nc-nd/4.0/>.

Introduction

Malignant mesothelioma is a rare and aggressive cancer type emerging from the mesothelium, which borders the surface of several organs, among which the lungs. Around 80% of all mesothelioma cases originate from the pleura, the mesothelial layer covering the lungs, and are called pleural mesothelioma (PM) [1]. PM is divided into three main subtypes based on its histomorphological growth pattern: epithelioid (55%), sarcomatoid (15%) and biphasic (30%), the latter having characteristics of both epithelioid and sarcomatoid PM.

The most important factor causing the development of PM is asbestos exposure, accounting for more than 80% of cases [2]. Inhaled asbestos fibres are deposited in the lungs and can cause chronic inflammation and frustrated phagocytosis, leading to DNA damage and tumour formation [3]. The latency period between first asbestos exposure and disease diagnosis is estimated to be 30–50 years. Describing the worldwide burden of PM is challenging, as there is invalid reporting and inaccurate diagnoses in many countries. At least 30,870 mesothelioma deaths worldwide were estimated in 2020, with the highest numbers in Northern Europe [4]. Due to the ban on the use of asbestos in several countries, the incidence rate has recently decreased for the first time [4]. Currently, the standard treatment has a palliative intent for most cases, and the prognosis is poor, with a median life expectancy of 10–12 months for untreated patients and 18 months for patients treated with immunotherapy [5].

The diagnosis of PM is difficult due to several reasons, including slow growth and non-specific presenting symptoms [6]. This results in an important diagnostic delay, often leading to diagnosis at an advanced disease stage. Moreover, PM is hard to differentiate from other benign or malignant lung-related diseases such as lung cancer. Currently, the initial diagnostic step for PM involves conducting a computed tomography (CT) scan [7, 8]. However, a chest CT scan is only able to visualize the tumour once it reaches a certain size [2]. The shape of a PM tumour also impedes visualization, because of its diffuse and non-spherical growth pattern along the lungs [9]. Moreover, conventional imaging methods, such as chest CT scans, are unreliable in distinguishing PM tumours from other benign asbestos-related lesions [2]. The histological examination of a biopsy sample by pathologists is the final challenging step towards the diagnosis of PM [10]. Initially, the cellular origin is determined using a targeted panel of mesothelial (e.g. WT1 and calretinin) and epithelial (e.g. MOC-31 and claudin-4) immunomarkers, for which sarcomatoid PM samples are negative [10, 11]. After confirmation of the mesothelial origin, histologic morphology is assessed. However, the morphologic overlap between PM and benign mesothelial

lesions complicates a reliable distinction. Therefore, additional immunohistochemical markers (e.g. for loss of *BAP1* and *MTAP* expression) and fluorescence in situ hybridization (e.g. for homozygous deletion of *CDKN2A*) are used to assist this decision [10]. Unfortunately, the absence of these specific markers is not consistent across all PM cases, thereby reducing the sensitivity of the diagnostic process. Another difficulty is both inter- and intra-tumour heterogeneity [8]. This diversity appears in both morphological and molecular dimensions. Molecular analyses elucidate notable heterogeneity among patients, within distinct regions of a given tumour concerning different clonal compositions, and throughout the treatment trajectory [12]. All these facts stress the need for biomarkers for early detection of PM with high specificity and sensitivity and for possible treatment allocation in case of an actionable target [6].

The field of tumour genetics is promising for the identification of novel biomarkers. Genetic alterations, including mutations in suppressor genes, such as *BAP1* (45.1%), *CDKN2A* (42.2%), *CDKN2B* (36.0%), *NF2* (31.3%), and *MTAP* (27.3%), have been reported in PM [13]. However, mutations are not suitable as general biomarkers for PM, as PM exhibits a heterogeneous genetic landscape and a low somatic mutational burden. Furthermore, no oncogenic driver mutations have been identified [14]. This could be explained by the fact that asbestos is a non-mutagenic carcinogen [15]. Therefore, interest in the epigenome has grown for the elucidation of tumour development and the identification of biomarkers [3]. The epigenome consists of histone modifications (including acetylation, methylation and phosphorylation) and DNA alterations (including methylation) without changing the genetic nucleotide sequence. An important epigenetic modification that is considered to be a hallmark of cancer is DNA methylation [16, 17].

DNA methylation involves the addition of a methyl group on the fifth position of cytosine in a CpG dinucleotide context, resulting in 5-methylcytosine [16]. Regions with a high frequency of CpG sites are called CpG islands and are often located in promoter regions of genes. In general, global epigenetic reprogramming is observed in all kinds of tumour types [17]. Overall, a global loss of methylation is detected in tumour cells, leading to genomic instability [17]. In contrast, hypermethylation of specific CpG islands can lead to gene silencing or inactivation, as observed in tumour suppressor genes. Conversely, hypomethylation of a CpG island in a promoter region can lead to gene activation or overexpression, potentially involving oncogenes [16]. Until now, most research has focused on DNA methylation of individual genes in PM [18]. Epigenome-wide analyses on PM samples have been sparse until two research groups

recently published DNA methylation analyses performed on a large cohort of PM patients [11, 19]. Bertero et al. aimed to discriminate PM from neoplastic and reactive histologic mimics, and Jurmeister et al. built a classification model to distinguish PM from chronic pleuritis, pleural carcinosis, and pleomorphic lung carcinomas. Neither research group included a control group comprising healthy pleural tissue samples. In this study we aimed to elucidate specific changes from healthy pleural tissue towards PM, necessitating the use of such a control group. Furthermore, variations in methylation patterns between PM and other lung-related diseases were studied. These alterations in DNA methylation patterns, when compared to those in pleural tissue and other lung diseases, hold the potential to serve as diagnostic biomarkers for PM.

Methods

Sample collection

PM tumour tissue samples were routinely collected between 2012 and 2021 by the biobank of the Antwerp University Hospital (UZA, Belgium). The UZA ethical committee approved our study and permitted the use of retrospective samples (Reference number 16/23/248). All tissue samples were fresh frozen and stored at -80°C after collection until further use. Diagnosis and overall tumour percentage were verified and determined by a pathologist (D.P.) by histological examination of hematoxylin–eosin-stained sections. We used 11 fresh frozen PM tumour tissue samples from treatment naïve patients, collected between 2013 and 2020. All samples had an overall tumour cell percentage (TCP) between 40 and 80% (Suppl Table S1).

For this study, 29 healthy parietal pleural tissue samples were prospectively collected from treatment naïve patients after approval of the UZA ethical committee (EDGE number 002046) in the Antwerp University Hospital in 2021 and 2022. The samples were collected from patients who underwent thoracic surgery for another reason than mesothelioma (Suppl Table S1). All patients gave written informed consent. All tissue samples were fresh frozen and stored at -80°C after collection until further use. The samples were verified by a pathologist (D.P.) by histological examination of hematoxylin–eosin-stained sections.

DNA extraction and methylation analysis

DNA was extracted from ten to fifteen $10\ \mu\text{m}$ -sections from the tissue samples, depending on the tissue size, using the QIAamp DNA Micro Kit (Qiagen, Hilden, Germany) according to the manufacturer's protocol. The DNA was stored at -20°C until further usage. 500 ng of each DNA sample was bisulfite converted with an EZ

DNA methylation kit (Zymo Research, California, USA) following the manufacturer's protocol specifically for a downstream analysis with an Infinium Methylation Microarray. Genome-wide methylation profiles were obtained using an Infinium Methylation EPIC 850 K BeadChip Kit both v1.0 and v2.0 (Illumina, California, USA) according to the manufacturer's protocol.

Methylation data processing and differential methylation analysis

Raw intensity array files were processed using the ChAMP (2.29.1) Bioconductor package [20, 21]. Methylation status was reported as Beta values, which range from 0 (indicating no methylation) to 1 (indicating full methylation). After data read-in, samples with more than 5% of their probed data missing were excluded. Underperforming probes were filtered out from the downstream analysis; this included control probes, X-/Y-chromosome probes, multihit probes, and probes with known single nucleotide polymorphisms (SNPs). The remaining probes with missing values were also removed and Beta values less than 0 were set at 0 and values above 1 were set at 1. To assess data quality, we calculated both the \log_2 median intensity ratios (for methylated and unmethylated signals) and the density of Beta values. To minimize technical discrepancies between Type-I and Type-II Illumina probes, BMIQ normalization was applied. Differential methylation was also conducted using ChAMP, which employs parametric linear mixed models to assess variations in methylation across different groups. The first criterion for identifying differentially methylated CpG sites (DMCs) was an adjusted P-value ($\text{adj.P.Val} \leq 0.05$, corrected for multiple testing using the Benjamini–Hochberg method [22]). The delta beta for each probe was defined as the difference in mean Beta value between group A and group B. A positive delta beta indicates higher methylation in group A (hypermethylation), while a negative delta beta reflects lower methylation in group A (hypomethylation). DMCs with an absolute delta beta value ≤ 0.05 were filtered out to reduce false positives. Lastly, we assessed the significance of batch effects across the CpG sites by comparing the fit of an ordinary least square regression model (with group as independent variable) without a random effect to that of a linear mixed model, incorporating batch as a random effect and group as a fixed effect. For each CpG site, we then tested whether the random effect was significant using a likelihood ratio test. Under the null hypothesis that no batch effect exist, the p -values from the random effect should follow a uniform $U(0,1)$ distribution. After calculating the significance of the random effect for all CpG sites, we compared the observed p -value distribution with the expected null distribution. CpG sites whose

p-value distribution deviated from the null were subsequently excluded from the final DMP list. Differentially methylated regions (DMRs) were identified using the Bumphunter algorithm extension in ChAMP. The significance of DMRs was determined based on the harmonic mean of the individual CpG *P*-values (FDR-corrected). DMRs with a mean difference ≤ 0.05 were filtered out to reduce false positives. All genomic locations are reported using Genome Build 19/ GRCh37.

Publicly available datasets

The MESOMICS Methylation EPIC 850 K (EGAD00010002053) and the LungNENomics Methylation EPIC 850 K (EGAD00010001720) datasets were downloaded from the European Genome-phenome Archive (EGA) after a Data Access Agreement with the owners [23, 24]. All other used datasets were downloaded from the Gene Expression Omnibus (GEO) and are listed in Table 1. To maintain uniform data processing, we chose to use raw idat files over processed beta values. The datasets were then processed using the same steps described above.

Statistical analyses

Subsequent analyses were carried out using the R software (version 4.3.1). For exploratory and visualization purposes, dimensionality reduction using *t*-distributed stochastic neighbour embedding (tSNE) clustering was performed using the Rtsne package with the 100,000 most variable probe Beta values. All adjusted *P*-values are two-sided, and those ≤ 0.05 were considered statistically significant. All genomic annotations were done using the GRCh37/hg19 genome build.

Results

Generation of the methylation data matrix

We performed a meta-analysis, combining our in-house generated EPIC methylation dataset consisting of 11 PM tissue samples and 29 healthy pleural tissue samples with 10 online available datasets of EPIC methylation data from PM and other lung diseases (Table 1). Collecting healthy pleural samples is challenging and to the best of our knowledge, this is the first time such a large dataset of healthy pleura samples has been generated. After quality control, 5 PM samples (dataset GSE164269) and 1 LUAD sample (dataset GSE203061) were excluded due to an excess of failed CpG sites (cut-off failed fraction of 0.05). Of the 865,917 examined CpG sites on the EPIC methylation array, 551,236 CpG sites have a successful measurement for each of the samples and were retained for further analysis (Suppl Table S2). The final data matrix consisted of DNA methylation data for 551,236 CpG sites on 257 pleural mesothelioma (PM) samples, 32 healthy pleura (PL) samples, 7 chronic pleuritis (CP) samples, 90 lung adenocarcinoma (LUAD) samples, 77 lung squamous cell carcinoma (LUSC) samples, 56 lung carcinoid (LUCA) samples, 20 large cell neuroendocrine carcinoma (LCNEC) samples, and 44 lung adjacent normal (LAN) samples.

Differential methylation between pleural mesothelioma and healthy pleura

First, we explored the methylation data of the PM and the healthy pleural tissue using a *t*-distributed stochastic neighbour embedding (tSNE) plot. Figure 1 displays a nearly perfect division between healthy pleura and PM samples. The healthy pleura samples are clustered closely

Table 1 Datasets and samples used in this study

Dataset	CP	LCNEC	LAN	LUAD	LUCA	LUSC	PL	PM	TOTAL
Own data							29	11	
EGAD00010001720 [24]		20			56				
EGAD00010002053 [23]							3	130	
GSE114989 [60]			7	27					
GSE124052 [61]						25			
GSE126043 [62]				9		6			
GSE158422 [63]			37			37			
GSE164269 [19]								79	
GSE175769 [64]								10	
GSE180060 [65]				27					
GSE203061 [11]	7			28		9		32	
TOTAL	7	20	44	91	56	77	32	262	589
After QC filtering	7	20	44	90	56	77	32	257	583

Bold indicates the total numbers are given before filtering and after QC filtering

CP, Chronic pleuritis; LAN, Lung adjacent normal; LCNEC, Large Cell Neuroendocrine Carcinoma of the Lung; LUAD, Lung adenocarcinoma; LUCA, Lung carcinoid; LUSC, Lung squamous cell carcinoma; PL, Pleura; PM, Pleural Mesothelioma

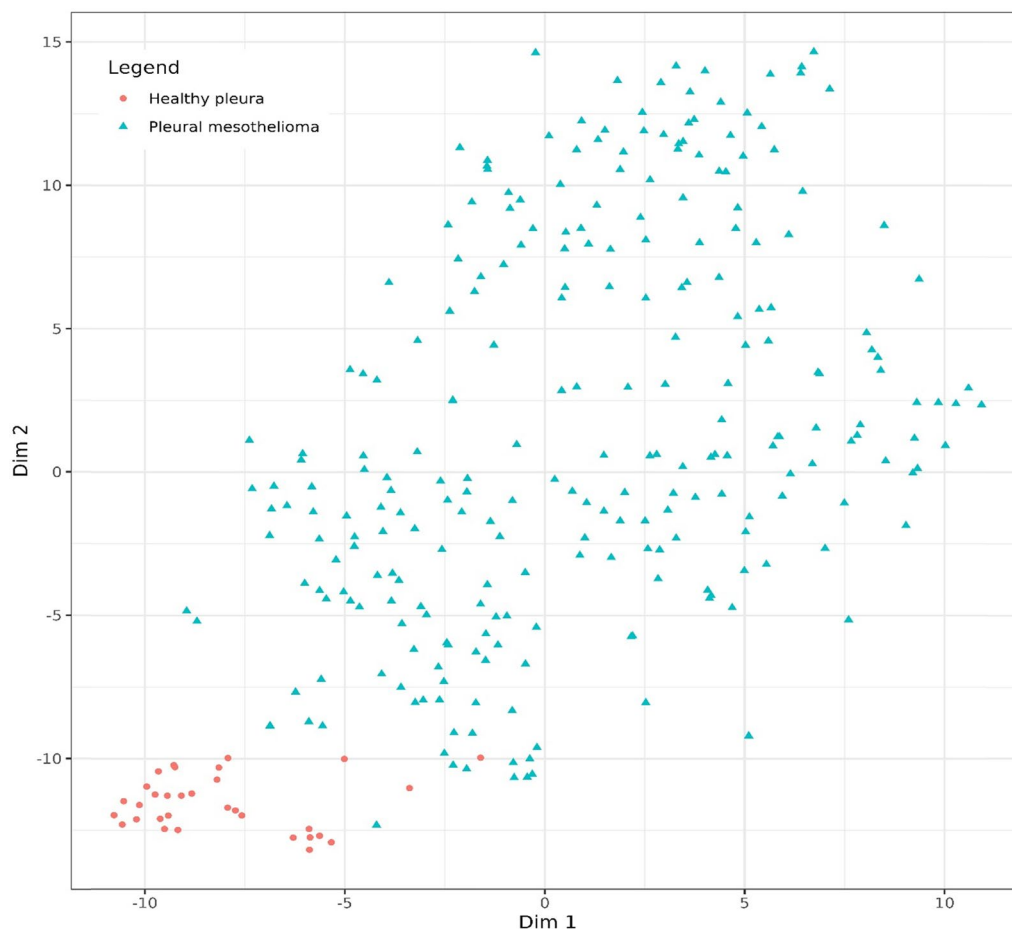


Fig. 1 t-distributed stochastic neighbour embedding (tSNE) plot of the methylation patterns based on the 100,000 most variable CpG sites of 257 PM samples and 32 healthy pleura samples

together, while the PM samples are more widespread. Three healthy pleura samples are visualized at the boundary of the PM cluster. We examined the association between tumour cell percentage (TCP) of each sample and the methylation pattern, but we found no correlation (Suppl Figure S1).

Differential methylation was identified in distinct genomic regions

Next, we investigated differential methylation patterns of individual CpG sites between PM tissue and healthy pleural tissue. Of the 551,236 examined CpG sites, we found 81,968 significantly differentially methylated CpG sites (DMCs). Of these, 50,346 are located in 14,745 unique protein-coding genes, 421 DMCs in 223 microRNA-coding genes, 1,178 DMCs in 569 lncRNA-coding genes and 30,023 in intergenic regions. For all DMCs, the difference in methylation level (delta beta) between the two groups was calculated. Of all DMCs, 63,463 CpG sites are hypomethylated in PM (negative delta beta), and 18,505 CpG

sites are hypermethylated in PM (positive delta beta). The only genomic locations with clear hypermethylation, are within CpG islands, especially in the intergenic regions (IGRs), in the 1500 bp and 200 bp fragment before the transcription start site (TSS200), the 5'UTR region, and the first exon (Fig. 2). In all other regions, hypomethylation predominates, especially in the open sea regions (i.e. not in proximity of CpG islands). Delta beta values range between -0.549 and 0.568 .

Most significant and differentially methylated CpG sites

To identify interesting CpG sites, we calculated two top 50 DMC lists, one ranked on adjusted P -value and one ranked on delta beta, as both parameters are essential for discrimination (Suppl Tables S3 and S4). Afterwards, we determined the overlap between both lists. This way, five CpG sites in four genes were identified: *MIR21*, *RNF39*, *SPEN* and *C1orf101* (Fig. 3 and Table 2). The area under the ROC curve (AUC) for the discrimination between

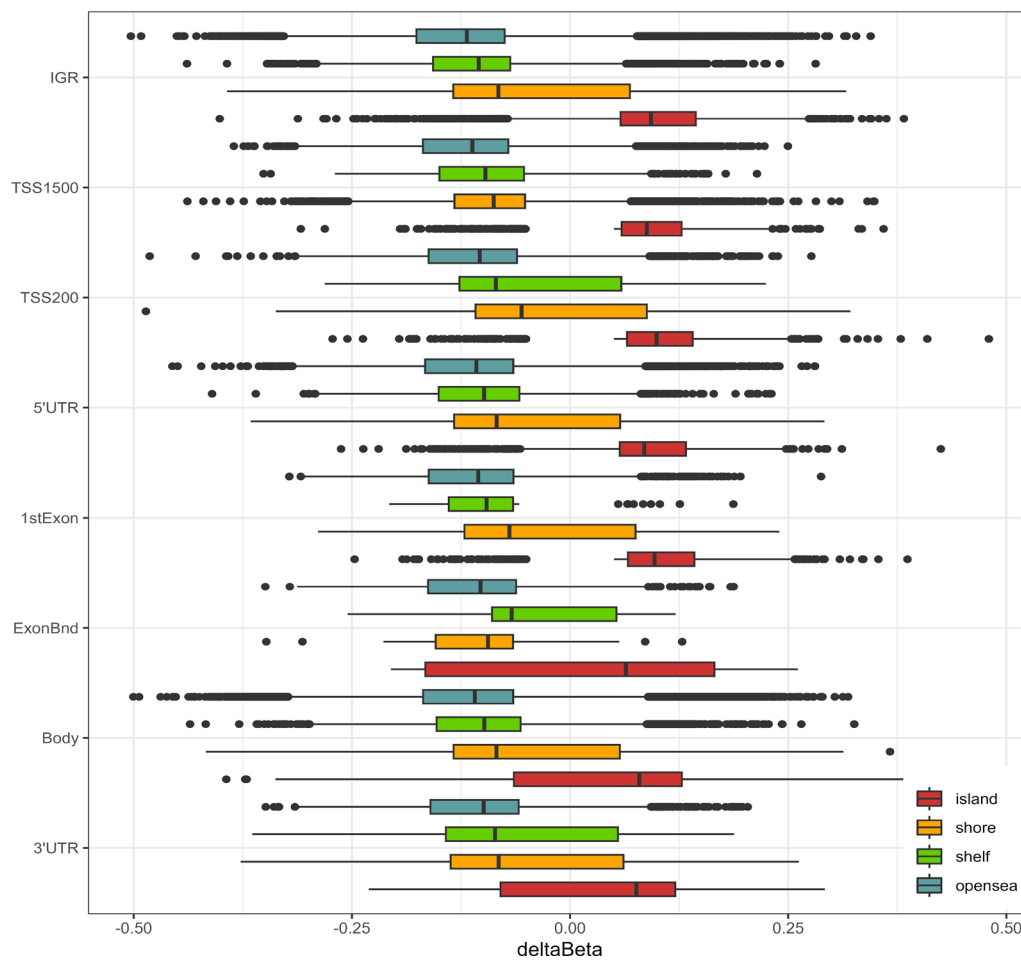


Fig. 2 Boxplot showing the delta beta distribution of each location category for all DMCs between PM and healthy pleura. Categories are based on genomic location (y-axis) and relation to a CpG island (colours). ExonBnd, exon boundaries; IGR, intergenic region; TSS, transcription start site; UTR, untranslated region

PM and healthy pleura for these DMCs ranges between 0.986 and 0.994.

We examined these four genes in more detail (Fig. 4). For *MIR21* (MicroRNA 21), all four examined CpG sites are hypomethylated and demonstrate a large delta beta (0.429, 0.482, 0.469 and 0.418). Two of them are located in the TSS200, the other two in the gene body. In *RNF39* (Ring Finger Protein 39), 28 of the 54 examined CpG sites are differentially methylated. There are 14 DMCs with a delta beta higher than 0.2 (hypermethylated). All of them are located in a CpG island at the end of the gene body. Notably, all DMCs in the promotor region are hypomethylated. However, in that region, no large delta beta values were detected. In *SPEN* (Spen Family Transcriptional Repressor), 11 of the 36 examined CpG sites are differentially methylated. Most of the DMCs are hypomethylated and DMCs with the highest absolute delta beta are located at the end of the gene body. In the promotor region, there is only one significant CpG site.

For *C1orf101* also known as *CATSPERE* (Catsper Channel Auxiliary Subunit Epsilon), seven of the 16 examined CpG sites are differentially methylated. Most of the DMCs are hypomethylated and DMCs with the highest absolute delta beta are located at the end of the gene body. In the promotor region, there is only one significant CpG site.

Comparison with COSMIC genes

We compared our list of DMCs with the COSMIC list (Catalogue of Somatic Mutations in Cancer) [25]. COSMIC presents a list of 743 genes with mutations causally implicated in cancer, including oncogenes, tumour suppressor genes, and fusion genes. Of this list, 677 genes are examined by the EPIC methylation array. Among the 81,968 DMCs we identified between PM and healthy pleura, 2,973 CpG sites are located in 556 COSMIC genes. For these genes, we calculated which ones have a high ratio of significant DMCs compared to the total

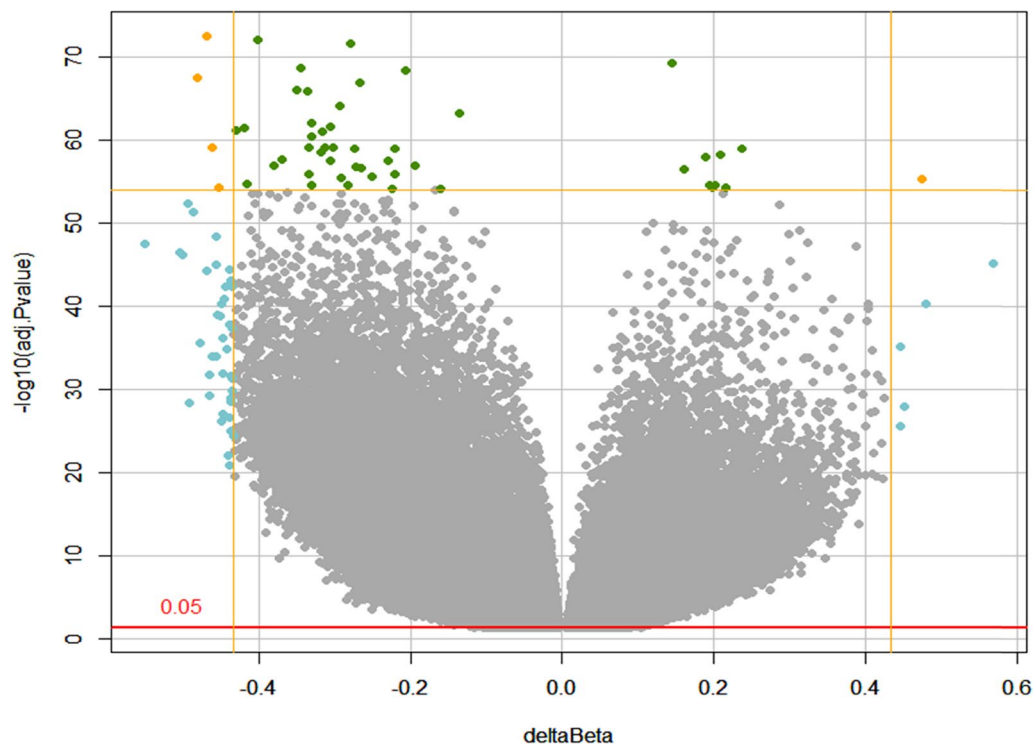


Fig. 3 Volcano plot showing delta beta (x-axis) and adjusted P -value (y-axis) for all 81,968 DMCs between PM and healthy pleura. The five overlapping DMCs of the top 50 for delta beta (blue) and adjusted P -value (green) are coloured orange

examined CpG sites for that gene, excluding genes with 10 or fewer examined CpG sites. One gene has a ratio of significant DMCs to examined CpG sites exceeding 0.5, which is *PDCD1LG2* (Programmed Cell Death 1 Ligand 2). Notably, all eight significant DMCs of *PDCD1LG2* are hypomethylated and are located in all regions of the gene (5'UTR, TSS1500, TSS200, first exon, and gene body).

Differentially methylated regions

In addition to analysing DMPs, we extended our investigation to differentially methylated regions (DMRs) between PM and healthy pleura. Through our analysis, we identified a total of 3,078 DMRs. Of these, 1,494 regions are hypermethylated in PM, while 1,584 regions are hypomethylated. To enhance the specificity of our findings, we applied a minimum cut-off value of 0.1 to the mean differential methylation. This more stringent criterion resulted in a refined list of 1,053 DMRs. Among these, the five most significant DMRs overlap with the genes *RNF39*, *SPEG*, *PISD*, *SEPT9*, and *PVT1*, respectively (Table 3).

Differential methylation between pleural mesothelioma subtypes

We compared the methylation patterns of the three PM subtypes: epithelioid ($n=157$), biphasic ($n=57$) and

sarcomatoid ($n=43$). In the tSNE plot (Fig. 5), the subtypes are not grouped in clearly separate clusters. However, the epithelioid PM and the sarcomatoid PM clusters are notably distinct from each other, whereas the biphasic PM samples cluster between the other two groups. Moreover, we found 182,840 DMCs between epithelioid and sarcomatoid PM, 93,871 DMCs between epithelioid and biphasic PM, and 52,139 DMCs between biphasic and sarcomatoid PM (Fig. 6A). The majority of the DMCs are hypermethylated in epithelioid PM compared to biphasic and sarcomatoid PM. The largest amount of DMCs are differentially methylated between epithelioid and sarcomatoid PM, and a large part of these DMCs ($n=61,825$) is also differentially methylated between epithelioid and biphasic PM (Fig. 6B). Of all DMCs between the subtypes, 9,157 are overlapping in each comparison, i.e. 9,157 CpG sites are significantly differentially methylated between each of the three groups.

Next, we compared the methylation level of the three subtypes separately with healthy pleura. We found 208,938 DMCs between pleura and epithelioid PM, 259,849 DMCs between pleura and biphasic PM, and 280,785 DMCs between pleura and sarcomatoid PM (Fig. 7A). The vast majority of these DMCs are hypermethylated in pleura compared to each of the PM subtypes. For the 9,157 overlapping DMCs between the

Table 2 The five overlapping DMCs of the top 50 ranked on delta beta and the top 50 ranked by adjusted P-value, between pleural mesothelioma (PM) and healthy pleura (PL)

CpG site	Adjusted P-value	Mean Beta in PM	Mean Beta in PL	Delta beta	Chr	Genomic location	Gene	Location gene	Location island	AUC
cg02515217	2.91E-68	0.121	0.603	-0.482	17	57,918,600	MIR21	TSS200	Open sea	0.989
cg06249604	4.57E-56	0.727	0.252	0.475	6	30,039,206	RNF39	Body	Island	0.994
cg15759721	2.82E-73	0.133	0.602	-0.469	17	57,918,630	MIR21	Body	Open sea	0.992
cg05099985	6.66E-60	0.305	0.768	-0.462	1	16,245,931	SPEN	Body	Open sea	0.986
cg20311002	6.22E-55	0.197	0.649	-0.452	1	244,763,541	C1orf101	Body	Open sea	0.988

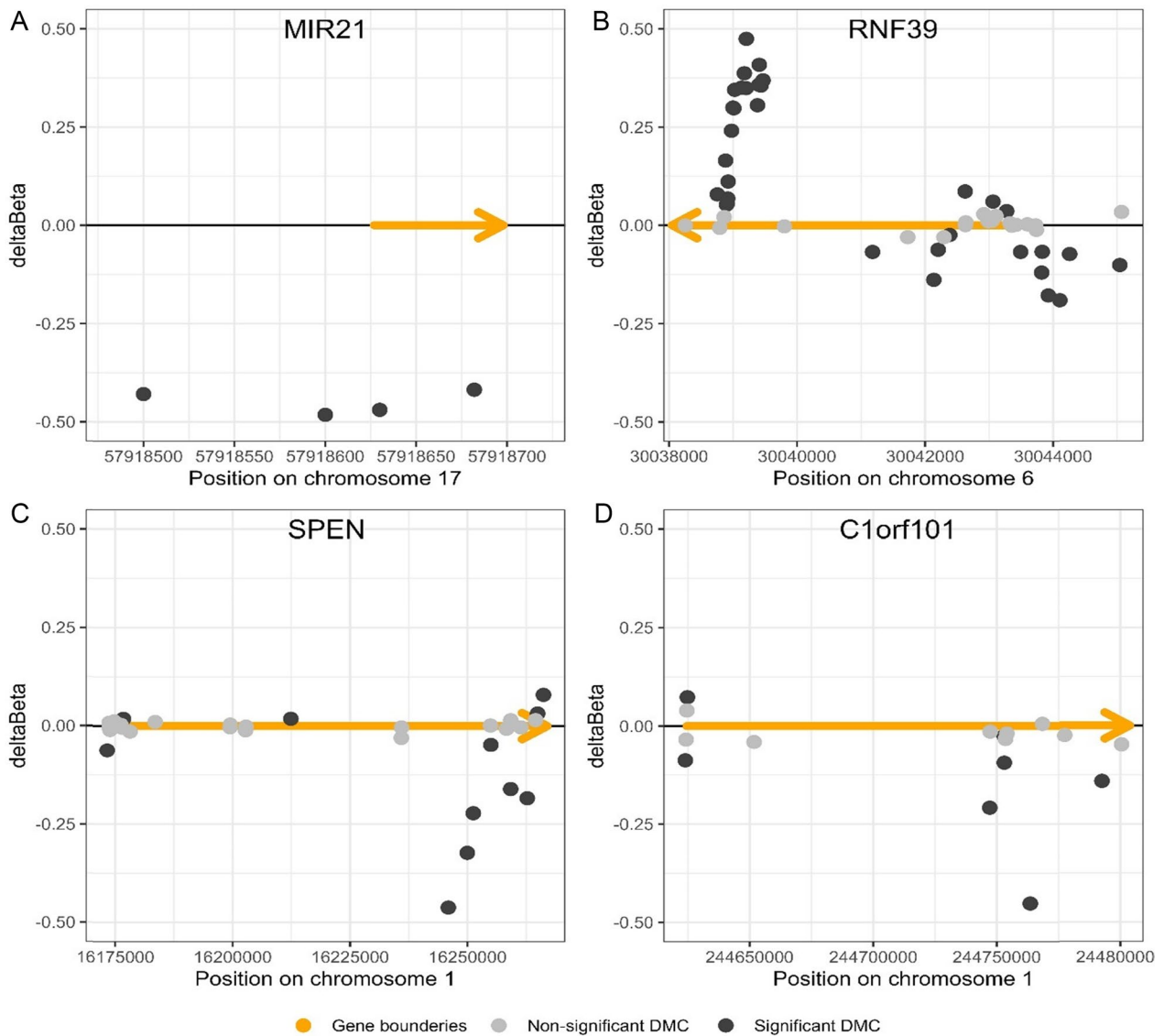


Fig. 4 Scatter plot showing the delta beta (difference in the methylation level) between PM and healthy pleura for each examined CpG site in the genes **A** *MIR21*, **B** *RNF39*, **C** *SPEN*, and **D** *C1orf101*. The dark grey points indicate the significantly methylated DMCs, the light grey points indicate the non-significant CpG sites and the orange arrow indicates the genomic location and the direction of transcription

Table 3 Five most significant differentially methylated regions between pleural mesothelioma and healthy pleura

Chrom	Start	Stop	Width	Number of CpGs	HMFDR	Maxdiff	Meandiff	Overlapping genes
chr6	30,038,254	30,039,466	1213	20	7,61E-34	0,474,573,918	0,229,528,006	<i>RNF39</i>
chr2	220,298,547	220,300,568	2022	13	2,79E-30	0,378,931,486	0,140,166,887	<i>SPEG</i>
chr22	32,057,065	32,058,810	1746	8	1,17E-27	-0,335,338,607	-0,173,441,195	<i>PISD</i>
chr17	75,281,339	75,284,193	2855	13	5,72E-26	-0,396,400,033	-0,230,612,988	<i>SEPT9</i>
chr8	128,806,271	128,808,554	2284	13	7,98E-26	-0,486,066,199	-0,181,561,728	<i>PVT1</i>

HMFDR: harmonic mean of the individual CpG *P*-values (FDR-corrected)

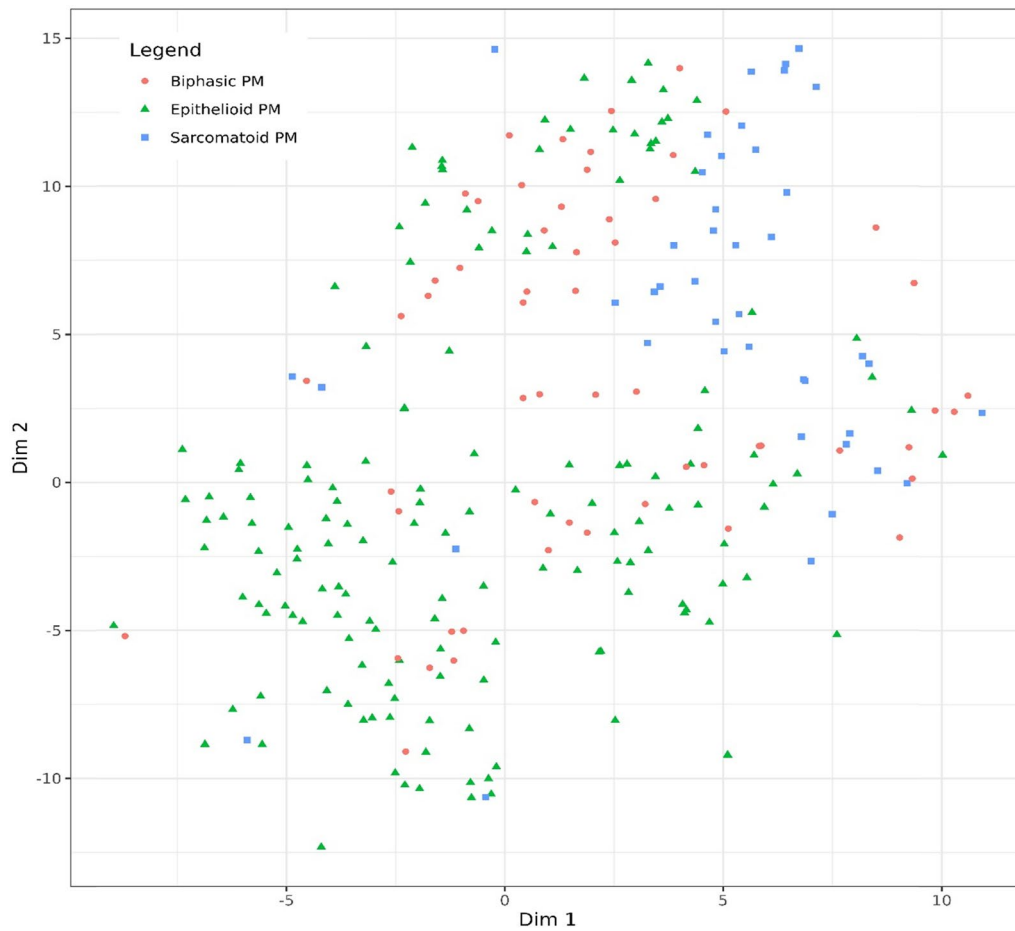


Fig. 5 t-distributed stochastic neighbour embedding (tSNE) plot of the methylation patterns based on the 100,000 most variable CpG sites of 157 epithelioid PM samples, 57 biphasic PM samples and 43 sarcomatoid PM samples

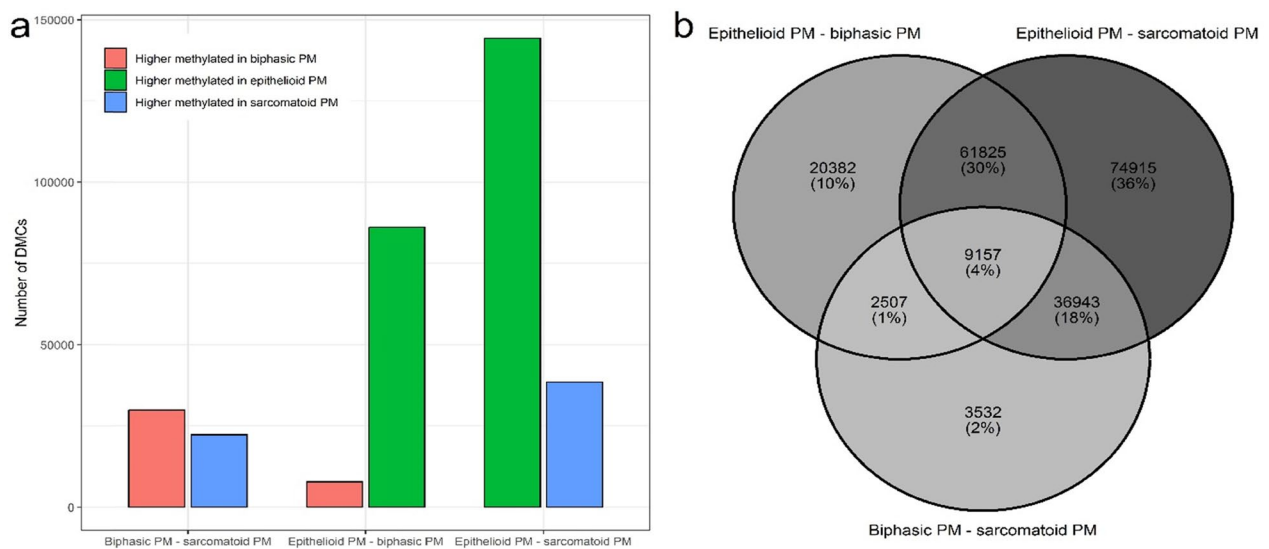


Fig. 6 Number of DMCs between the three PM subtypes. **a** Barplot showing the numbers of DMCs higher methylated in each of the subtypes and each of the comparisons. **b** Venn diagram showing the overlapping DMCs in each of the comparisons. The darker the grey, the higher the amount of DMCs

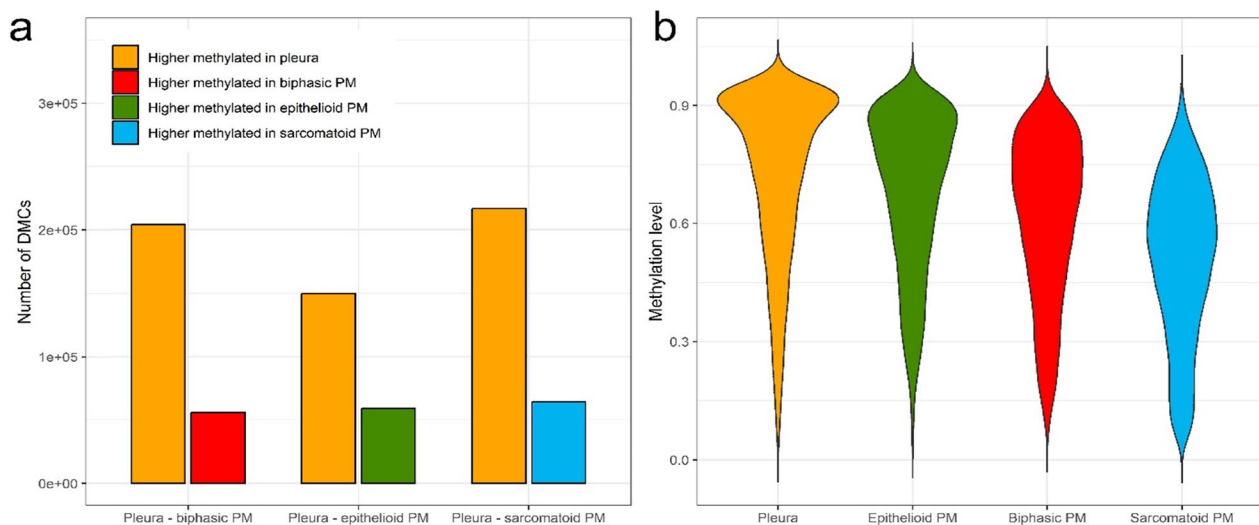


Fig. 7 **a** Barplot showing the numbers of DMCs higher methylated in each of the subtypes or healthy pleura, and each of the comparisons. **b** Violin plot showing the distribution of the methylation levels in each of the subtypes and healthy pleura for the 9,157 overlapping DMCs between the subtypes

subtypes, the distribution of the methylation levels for the three subtypes and healthy pleura is shown in a violin plot (Fig. 7B). This plot shows clearly that the methylation levels are highest in healthy pleura, lower in epithelioid PM, even lower in biphasic PM, and lowest in sarcomatoid PM.

Differential methylation between pleural mesothelioma and other lung diseases

We compared the methylation pattern of PM with those from the other lung-related samples (PL, CP, LUAD, LUSC, LUCA, LCNEC, LAN), aiming to detect tissue and tumour type-specific methylation patterns. In the tSNE plot (Fig. 8), most of the groups form a clear cluster. In dimension 1, the pleura-related samples are perfectly distinguishable from lung-related samples, while dimension 2 discriminates based on the disease state. For each comparison, the number of DMCs was calculated (Suppl Table S5). More than 70,000 DMCs were identified for each comparison, except for the comparison with chronic pleuritis, where 13,834 DMCs were detected. Of all DMCs, 2,204 CpG sites are differentially methylated between PM and each of the other groups. In a violin plot showing the average methylation levels of those common DMCs for each of the groups (Fig. 9), it is evident that most of these DMCs are hypomethylated in PM, as the density of PM is much higher around a methylation level of 0.4, while in all other groups, the methylation level is denser for higher values.

Discussion

Pleural mesothelioma is a rare and rapidly fatal disease, with asbestos exposure standing out as the foremost risk factor contributing to its development. Previous research has demonstrated the presence of somatic mutations in PM [13]. However, PM exhibits a relatively low number of pathogenically significant mutations [26]. Therefore, the epigenome is now extensively being investigated. The precise mechanism behind the prominence of epigenetic alterations in PM remains elusive. However, it is widely recognized that chronic inflammation is a primary response to asbestos exposure. Notably, epigenetic modifications have been closely associated with inflammatory processes in other cancers [27]. This suggests that inflammation-related epigenetic changes may play an important role in various human cancers, including pleural mesothelioma.

Currently, the investigation of genome-wide methylation changes from healthy pleura to PM has been limited. Our study aims to further elucidate the epigenetic landscape of PM. Surprisingly, widespread differential methylation between PM and healthy pleura was observed, considering that we detected 81,968 differentially methylated CpG sites. These DMCs are located in all genomic regions, including noncoding RNA, which is perhaps not surprising as methylation also plays an important role in the regulation of noncoding RNA transcription, in addition to protein-coding genes [28]. MiRNAs and lncRNAs are regulators of cellular processes such as differentiation and proliferation, and aberrant methylation of these types of RNA can lead to cancer development

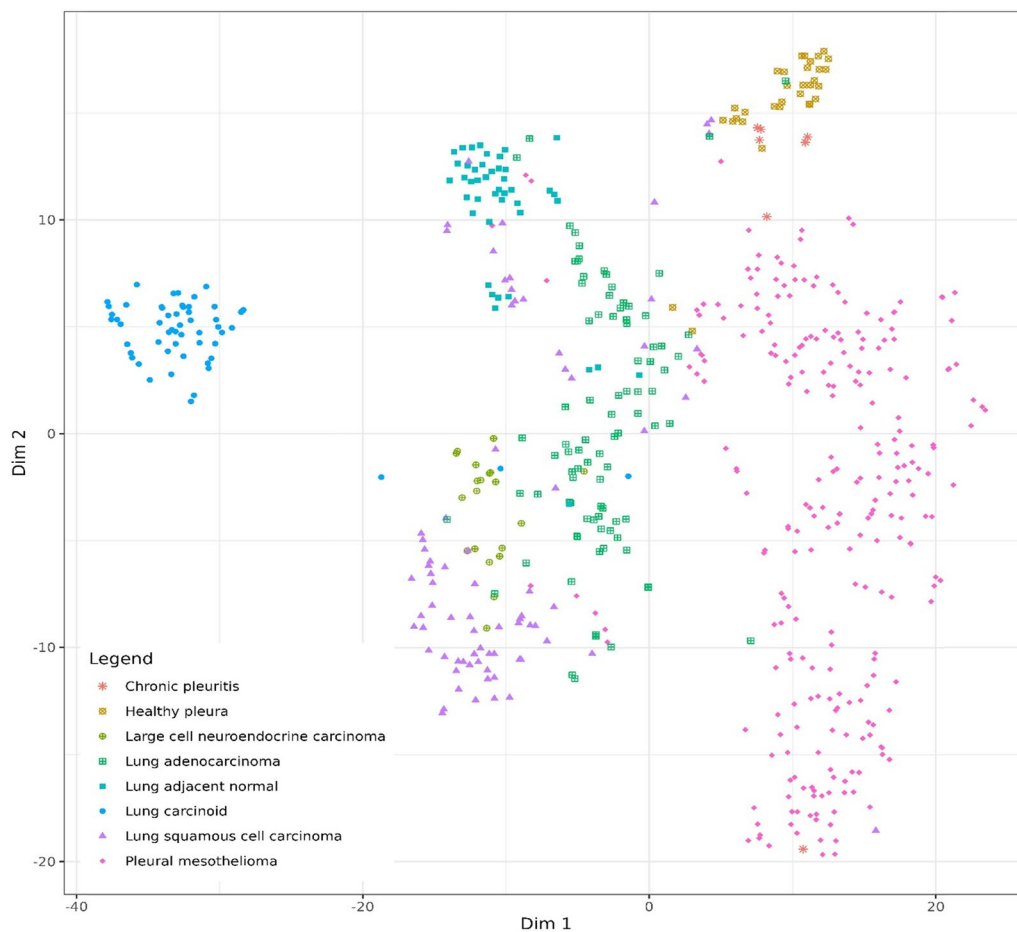


Fig. 8 t-distributed stochastic neighbour embedding (tSNE) plot of the methylation patterns based on the 100,000 most variable CpG sites of 257 PM samples, 32 healthy pleura samples, 7 chronic pleuritic samples, 90 lung adenocarcinoma samples, 77 lung squamous cell samples, 56 lung carcinoid samples, 20 large cell neuroendocrine carcinoma samples, and 44 lung adjacent normal samples

[28]. Unfortunately, the noncoding genomic regions are underrepresented on the EPIC methylation array, despite being crucial in the epigenetic regulation. This is due to a selection process primarily focusing on genes implicated in cancer. This obstacle could potentially be addressed through future implementation of genome-wide ONT sequencing. Unexpectedly, a large number of DMCs was found in intergenic regions. It is still unclear whether these aberrations are tumour-causing or a consequence.

Actively transcribed genes in healthy human cells are known to have unmethylated promoters, especially when they contain a CpG island, and slightly methylated gene bodies [28]. In tumour cells, however, a global loss of DNA methylation is described in several studies. On the other hand, CpG islands and shores in gene promoters are often hypermethylated in tumoural DNA, resulting in gene silencing of tumour suppressor genes [28, 29]. Roughly 50% of all human genes harbour CpG islands, and are therefore susceptible to this type of aberrant

silencing [30]. Moreover, hypomethylation of promoter regions without CpG island has been observed as well and can result in overexpression of oncogenes and proto-oncogenes, although this occurs less frequently [28]. This is in agreement with our observations (Fig. 2). When comparing healthy pleura to PM, the only hypermethylated locations are the CpG islands (in all gene locations and IGRs). Other locations are hypomethylated in all gene locations and IGRs.

Christensen et al. performed a genome-wide methylation analysis comparing PM samples with healthy pleura [15]. However, they investigated only 1505 CpG sites associated with 803 cancer-related genes using the Illumina GoldenGate BeadArray technology and compared 158 PM samples to only 18 healthy pleura samples. They identified 969 CpG sites in 646 genes that are aberrantly methylated in mesothelioma samples. Of these genes, two overlap with our Top 50 DMCs ranked on delta beta: *FHIT* and *PLXDC2*. Surprisingly, in our analysis, *FHIT*

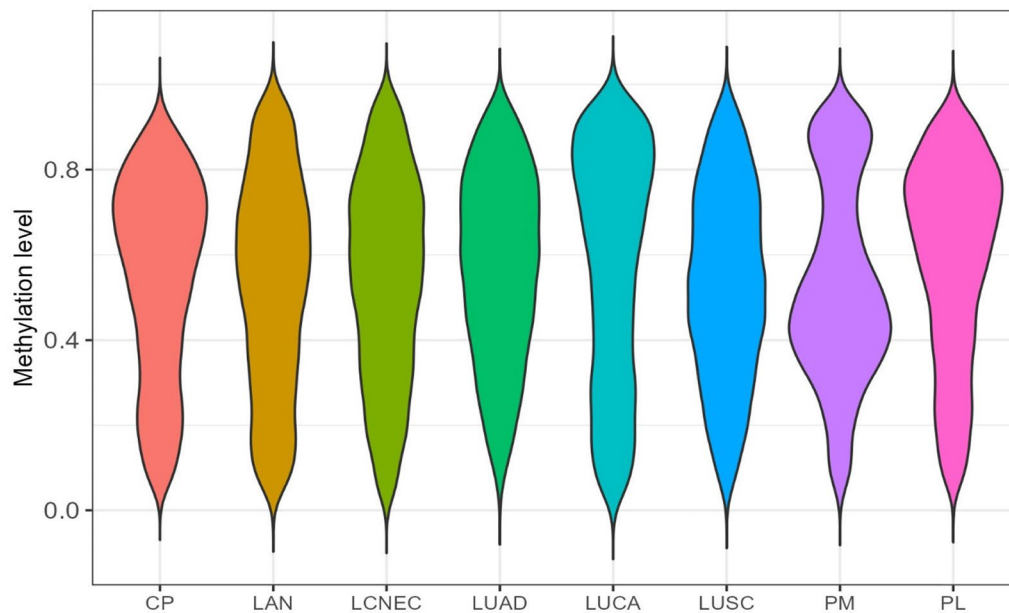


Fig. 9 Violin plot showing the distribution of the methylation levels in PM and other lung-related samples for the 2,204 overlapping DMCs between all the groups. CP, Chronic pleuritis; LAN, Lung adjacent normal; LCNEC, Large Cell Neuroendocrine Carcinoma of the Lung; LUAD, Lung adenocarcinoma; LUCA, Lung carcinoid; LUSC, Lung squamous cell carcinoma; PM, Pleural Mesothelioma; PL, Pleura

has a hypermethylated CpG site in PM (in the promoter region), while in Christensen's study, *FHIT* has two hypomethylated CpG sites (one in the promoter and one in the body). The Fragile Histidine Triad Diadenosine Triphosphatase (*FHIT*) gene encodes for a triphosphate hydrolase that is involved in purine metabolism. In addition, *FHIT* is a tumour suppressor gene crucial for DNA repair, cell cycle regulation, and apoptosis. It has been suggested to be a target of lung carcinogens, such as tobacco smoke and asbestos [31]. *FHIT* has been described to have a reduced protein expression in PM [32, 33]. In childhood acute lymphoblastic leukaemia, *FHIT* is defined to have both promoter hypermethylation and reduced mRNA expression [34]. *PLXDC2* encodes for Plexin Domain Containing-Protein 2 and is also known as *TEM7R* (tumour endothelial marker 7-related). In both studies, *PLXDC2* is hypomethylated. Dysregulation of *PLXDC2* is associated with cancer progression and metastasis via roles in angiogenesis, cell migration, and invasion, for example in gastric cancer [35]. However, *PLXDC2* has never been linked with mesothelioma before.

We selected four genes for a more detailed examination. *MIR21* encodes for a microRNA which is a small RNA fragment that regulates gene expression of several genes at post-transcriptional level [36]. *MIR21* has been described earlier to be over-expressed in PM [37]. This corresponds to our finding that the TSS200 of the *MIR21* gene is hypomethylated in PM [38]. MicroRNAs

are described to be stable in body fluids and as such have potential as biomarkers [39]. Expression of *MIR21* is also been described to be a potential prognostic biomarker for PM [40]. However, a recent review describes how *MIR21* is claimed to be a predictive or prognostic biomarker for at least 29 diseases [39]. This knowledge undermines the potential of *MIR21* as a specific biomarker for PM.

RNF39 encodes for Ring Finger Protein 39 which is suggested to play a role in an early phase of synaptic plasticity and has potential E3 ubiquitin ligase activity [41]. The altered expression of *RNF39* is described to be a potential prognostic biomarker for cholangiocarcinoma and pancreatic cancer [42, 43]. The *RNF39* gene is located in a significantly hypomethylated region in peripheral blood mononuclear cells of breast cancer patients with DOX-induced cardiotoxicity [44]. Further, little is known about the functions of this gene in cancer [43].

SPEN encodes for Spen Family Transcriptional Repressor which is a hormone-inducible transcriptional repressor and is mainly involved in X chromosome inactivation [45]. It is also known as SMART/HDAC1-associated repressor (*SHARP*) [46]. A recent study describes the potential of *SPEN* mutations as a predictive biomarker for immunotherapy in a pan-cancer analysis [45]. Another study describes *SPEN* as a tumour suppressor gene and a candidate predictive biomarker in ER α -positive breast cancers [47]. However, until now no association between this gene and PM has been described.

C1orf101 is also known as *CATSPERE* and encodes for Catsper Channel Auxiliary Subunit Epsilon. This is an auxiliary component of the CatSper complex, a complex involved in sperm cell hyperactivation. A recent study identified *CATSPERE* as a mediator of colorectal cancer susceptibility and progression [48]. Furthermore, no associations of this gene with cancer are described.

DNA methylation occurs early in tumour development and can be detected in body fluids [29]. Therefore, it is an ideal source for biomarkers. The aberrant methylation that we identified in this study, can be further investigated as a potential diagnostic biomarker for the detection of PM. The five CpG sites we elucidated (Table 2) have an AUC ranging between 0.986 and 0.994, and therefore have high biomarker potential. In addition to biomarkers, DNA methylation could also be a source of therapeutic targets. DNA methylation is reversible and methyltransferase inhibitors, such as 5'-azacytidine, are currently being used to treat several cancer types, including acute myeloid leukaemia [29, 49]. Understanding the functional roles of particular genes in the context of PM pathogenesis could offer valuable insights into the underlying molecular mechanisms driving this aggressive cancer and may hold promise for the development of novel targeted therapies.

We analysed our findings in the light of established knowledge about cancer in general and PM specifically. The COSMIC database, which catalogues mutations, copy number alterations and other genomic changes in cancer, provides a valuable reference for our study. Notably, of the cancer genes listed in COSMIC with CpG sites examined by the EPIC array, 82% (556/677) exhibited altered methylation in PM. This suggests that methylation changes in PM are more ubiquitous than mutations, extending across the entire genome rather than being confined to a few driver mutations.

In addition to analysing DMPs, we examined DMRs between PM and healthy pleura to gain a broader perspective on epigenetic regulation. While cancer cells are generally more hypomethylated than normal cells, as confirmed by our DMP analysis, we observed an almost equal number of hypermethylated and hypomethylated DMRs. This suggests a complex and nuanced landscape of epigenetic regulation in PM cells. Although global hypomethylation is a common feature, these results indicate that epigenetic changes in PM are not uniform. They involve both the silencing of key regulatory genes through hypermethylation and the activation or destabilization of other regions through hypomethylation. Notably, the five most significant DMRs overlap with the genes *RNF39*, *SPEG*, *PISD*, *SEPT9*, and *PVT1*. The DMR overlapping *RNF39* corresponds to the end of the gene body (width of 1213 bp), where we also identified

several DMPs (Fig. 4). Surprisingly, the DMR overlapping *SEPT9* (Septin 9) is hypomethylated, even though *SEPT9* is frequently described as a hypermethylated biomarker in colorectal cancer and other cancer types [50, 51]. Long noncoding RNA plasmacytoma variant translocation 1 (*PVT1*) has been identified as playing an important role in cancer development as oncogene [52]. However, the genes *SPEG* and *PISD* have not been previously linked to cancer.

When comparing the methylation patterns of the three PM subtypes, no explicit separation can be visualized by clustering. However, a clear trend is observed in the methylation levels of the subgroups and healthy pleura (Fig. 7). The highest methylation levels are detected in healthy pleura, followed by epithelioid PM, subsequently biphasic PM, and finally, sarcomatoid PM, in which the lowest methylation levels are observed. Increased hypomethylation observed in tumours is often associated with more aggressive and malignant disease phenotypes [53]. This hypomethylation can lead to the activation of oncogenes and to genomic instability, which contributes to tumour progression and aggressiveness. Studies have shown a correlation between the extent of hypomethylation in other tumours and the severity of the disease, including increased invasiveness, metastatic potential, and resistance to therapy [54, 55]. Global DNA hypomethylation is also associated with a detrimental prognosis in tumour patients [56]. This is consistent with our findings, as sarcomatoid PM is described to have more distant metastases than other PMs, and has the worst prognosis [57]. Moreover, differential methylation between the PM subgroups could potentially be used for PM subclassification. This was already demonstrated on central nervous system tumours, for which the application of DNA methylation-based classification has been demonstrated in a routine diagnostic setting [58].

Based on the methylation patterns, PM can be accurately distinguished from other lung-related diseases. For all comparisons, we reported more than 70,000 DMCs except when compared to chronic pleuritis. Chronic pleuritis, also known as chronic inflammation of the pleura, is not universally recognized as a precursor stage of mesothelioma. While chronic inflammation can sometimes precede the development of mesothelioma, it does not necessarily indicate a direct progression from chronic pleuritis to mesothelioma in all cases. The relationship between chronic pleuritis and mesothelioma is complex and may involve various contributing factors beyond inflammation alone. Therefore, it is important for individuals with chronic pleuritis and a history of asbestos exposure to undergo regular medical evaluation and monitoring for the potential development of mesothelioma. Although only 13,834 DMCs were identified

between chronic pleuritis and PM, we believe that the small sample size of the chronic pleuritis group ($n=7$) resulted in the lack of power to identify more DMCs. Studies with larger sample sizes are needed to validate the potential to discriminate PM from chronic pleuritis based on the methylation pattern. One remarkable observation is the differential methylation in the *RNF39* gene between PM and chronic pleuritis. Five CpG sites of the top 10 DMCs ranked on delta beta are located in the *RNF39* gene (Suppl Table S6). The end of the gene body is extremely hypermethylated in PM compared to chronic pleuritis (Suppl Figure S2), which is very similar to Fig. 4B in which PM is compared to healthy pleura.

In addition to biomarkers differentiating PM from healthy pleura, it could become even more interesting when biomarkers can be identified to distinguish PM from similar diseases to improve diagnostic accuracy. Especially differentiation from different types of lung cancer is important, as these can present with similar symptoms, such as chest pain, shortness of breath, and coughing. Additionally, both PM and lung cancer can result from exposure to carcinogens, such as asbestos. Moreover, radiographic findings can overlap between PM and other lung cancers, with features such as pleural thickening, pleural effusion, and mass lesions within the lung or pleura. Finally, these similar disease entities frequently show the same expression of pathologic immunohistochemical markers as PM, which complicates diagnosis and may even result in the wrong diagnosis. DNA methylation profiles are very robust and disease-specific and could potentially resolve all mentioned difficulties for the diagnosis of lung diseases, leading to appropriate treatment planning and management for the correct diagnosis.

Differences in genome-wide methylation patterns between PM and lung cancer were already described by several research groups. Goto et al. conducted a comparison of 6157 CpG islands in 20 PM samples with 20 LUAD samples using methylated CpG island amplification microarray analysis [59]. Across all samples, an average of 387 genes exhibited hypermethylation in PM, whereas 544 genes showed hypermethylation in LUAD. Among the most noteworthy hypermethylated genes in PM were *TMEM30B*, *KAZALD1*, and *MAPK13*. Notably, these genes were unmethylated in LUAD samples, confirming their specificity for PM [59]. Bertero et al. utilized EPIC methylation arrays to analyse the methylation patterns of 79 PM samples in comparison to 202 cases representing malignant and benign diagnostic mimics [19]. Employing both unsupervised hierarchical clustering and t-distributed stochastic neighbour embedding analysis, PM samples exhibited a distinct DNA methylation profile compared to other neoplastic and reactive mimics [19].

Jurmeister et al. utilized both 450 K and EPIC methylation arrays to compare the methylation patterns among 196 PM, 507 LUAD, 413 LUSC, and 17 CP samples [11]. Through the application of two machine learning algorithms, the study attained high accuracies using their support vector machine (97.8%), while their random forest model exhibited lower performance (89.5%), particularly in distinguishing PM from CP. Furthermore, differential methylation analysis uncovered promoter hypermethylation in PM specimens, implicating tumour suppressor genes such as *BCL11B*, *EBF1*, *FOXA1*, and *WNK2* [11].

Conclusion

In conclusion, the analysis of DNA methylation patterns emerges as a promising avenue for differentiation between various tissue and tumour types. The substantial number of methylation alterations observed between healthy pleura and PM underscores the importance of these epigenetic changes in the pathogenesis of the disease. These alterations could be used as biomarkers or molecular targets for therapy. Additionally, the ability to distinguish between different subtypes of PM based on their unique methylation profiles offers valuable insights for personalized diagnostic and therapeutic interventions as well as prognosis. Finally, the distinct methylation signatures exhibited by PM compared to other lung cancers highlight the potential of methylation profiling as a diagnostic tool in the clinical setting. Translational studies need to be conducted to enable the utilization of this methylation signature in clinical settings.

Supplementary Information

The online version contains supplementary material available at <https://doi.org/10.1186/s13148-024-01790-z>.

Additional file 1.

Additional file 2.

Acknowledgements

We would like to extend our sincere gratitude to the patients and surgeons whose generosity made this research possible by providing the necessary samples. Special thanks are also due to Anne Schepers for her execution of the sample processing, which was instrumental to the success of this study. Additionally, we express our appreciation to Tycho Cremers for his technical and bio-informatic support, which significantly contributed to the analysis of our data. Finally, we would like to thank Thomas Vanpoucke for submitting our methylation data to the EGA database.

Author contributions

JV contributed to conceptualization of the study, methodology, interpreting results, writing original draft, reviewing and editing of the final draft; JI and NDM contributed to methodology, interpreting results, reviewing and editing of the final draft; DP, JR, JH and PVS contributed to methodology, reviewing and editing of the final draft; JVM contributed to conceptualization of the study, reviewing and editing of the final draft. GVC and KODB contributed to conceptualization of the study, interpreting results, reviewing and editing of

the final draft. All authors have read and agreed to the published version of the manuscript.

Funding

Mesothelioma research in the lab of Prof. Guy Van Camp is supported by grants awarded by the University of Antwerp (IOF/SBO 43782 and BOF/TOP 39705) and the Stichting Tegen Kanker (STK 46773).

Availability of data and materials

Methylation data have been deposited at the European Genome-phenome Archive (EGA), which is hosted by the EBI and the CRG, under accession number EGAS00001007783. Further information about EGA can be found on <https://ega-archive.org>.

Declarations

Ethical approval and consent to participate

This study was conducted in accordance with Good Clinical Practice guidelines and the Declaration of Helsinki. Fresh frozen PM tissue samples used in this study were previously collected in the Biobank of the Antwerp University Hospital and retrospectively used in this study which was approved by the UZA ethical committee (Reference number 16/23/248). According to Article 20 of the Belgian Law on the procurement and use of human corporal material intended for human application or scientific research of 19 December 2008, patients provide consent for the use of their bodily material in research when consenting to an invasive procedure. As such, no additional consent was needed for the use of these retrospective samples. For prospectively collected healthy pleural tissue samples, written informed consent was given by each subject. The study protocol was approved by the UZA ethical committee (EDGE number 002046) before experimental analyses were performed.

Consent for publication

Not applicable.

Competing interests

The authors declare no competing interests.

Author details

¹Centre of Medical Genetics, University of Antwerp and Antwerp University Hospital, Edegem, Belgium. ²Centre for Oncological Research Antwerp (CORE), University of Antwerp and Antwerp University Hospital, Wilrijk, Belgium. ³Department of Pathology, Antwerp University Hospital, Edegem, Belgium. ⁴Department of Thoracic Oncology, Antwerp University Hospital, Edegem, Belgium. ⁵Department of Thoracic and Vascular Surgery, Antwerp University Hospital, Edegem, Belgium. ⁶Antwerp Surgical Training, Anatomy and Research Centre (ASTARC), University of Antwerp, Wilrijk, Belgium.

Received: 18 April 2024 Accepted: 20 November 2024

Published online: 03 December 2024

References

- Kim RY, Sterman DH, Haas AR. Malignant mesothelioma: has anything changed? *Semin Respir Crit Care Med*. 2019;40:347–60.
- van Meerbeeck JP, Hillerdal G. Screening for mesothelioma. *Am J Respir Crit Care Med*. 2008;178:781–2.
- Christensen BC, et al. Asbestos exposure predicts cell cycle control gene promoter methylation in pleural mesothelioma. *Carcinogenesis*. 2008;29:1555–9.
- Huang J, et al. Global incidence, risk factors, and temporal trends of mesothelioma: a population-based study. *J Thorac Oncol*. 2023;18:792–802.
- Baas P, et al. First-line nivolumab plus ipilimumab in unresectable malignant pleural mesothelioma (CheckMate 743): a multicentre, randomised, open-label, phase 3 trial. *Lancet*. 2021;397:375–86.
- Cioce M, et al. Protumorigenic effects of mir-145 loss in malignant pleural mesothelioma. *Oncogene*. 2014;33:5319–31.
- Baas P. Predictive and prognostic factors in malignant pleural mesothelioma. *Curr Opin Oncol*. 2003;15(2):127–30.
- Popat S, et al. Malignant pleural mesothelioma: ESMO clinical practice guidelines for diagnosis, treatment and follow-up. *Ann Oncol*. 2022;33:129–42.
- Scherpereel A, Lee YG. Biomarkers for mesothelioma. *Curr Opin Pulm Med*. 2007;13:339–43.
- Chapel DB, Schulte JJ, Husain AN, Krausz T. Application of immunohistochemistry in diagnosis and management of malignant mesothelioma. *Transl Lung Cancer Res*. 2020;9:53.
- Jurmeister P, et al. DNA methylation-based machine learning classification distinguishes pleural mesothelioma from chronic pleuritis, pleural carcinosis, and pleomorphic lung carcinomas. *Lung Cancer*. 2022;170:105–13.
- Oehl K, Vrugt B, Opitz I, Meerang M. Heterogeneity in malignant pleural mesothelioma. *Int J Mol Sci*. 2018;19(6):1603.
- Hiltbrunner S, et al. Genomic landscape of pleural and peritoneal mesothelioma tumours. *Br J Cancer*. 2022;127:1997–2005.
- Hmeljak J, et al. Integrative molecular characterization of malignant pleural mesothelioma. *Cancer Discov*. 2018;8:1549–65.
- Christensen BC, et al. Epigenetic profiles distinguish pleural mesothelioma from normal pleura and predict lung asbestos burden and clinical outcome. *Cancer Res*. 2009;69:227–34.
- Tsou JA, et al. Distinct DNA methylation profiles in malignant mesothelioma, lung adenocarcinoma, and non-tumor lung. *Lung Cancer*. 2005;47:193–204.
- Ibrahim J, Op de Beeck K, Franssen E, Peeters M, Van Camp G. Genome-wide DNA methylation profiling and identification of potential pan-cancer and tumor-specific biomarkers. *Mol Oncol*. 2022. <https://doi.org/10.1002/1878-0261.13176>.
- Vandenhoeck J, et al. DNA methylation as a diagnostic biomarker for malignant mesothelioma: a systematic review and meta-analysis. *J Thorac Oncol*. 2021. <https://doi.org/10.1016/j.jtho.2021.05.015>.
- Bertero L, et al. DNA methylation profiling discriminates between malignant pleural mesothelioma and neoplastic or reactive histologic mimics. *J Mol Diagn*. 2021;23:834–46.
- Morris TJ, et al. ChAMP: 450k chip analysis methylation pipeline. *Bioinformatics*. 2014;30:428–30.
- Fortin JP, Triche TJ Jr, Hansen KD. Preprocessing, normalization and integration of the Illumina HumanMethylationEPIC array with minfi. *Bioinformatics*. 2017;33(4):558–60.
- Glueck DH, Mandel J, Karimpour-Fard A, Hunter L, Muller KE. Exact calculations of average power for the Benjamini-Hochberg procedure. *Int J Biostat*. 2008. <https://doi.org/10.2202/1557-4679.1103>.
- Genova AD, et al. A molecular phenotypic map of malignant pleural mesothelioma. *Gigascience*. 2022. <https://doi.org/10.1093/gigascience/giac128>.
- Alcala N, et al. Integrative and comparative genomic analyses identify clinically relevant pulmonary carcinoid groups and unveil the supra-carcinoids. *Nat Commun*. 2019. <https://doi.org/10.1038/s41467-019-11276-9>.
- Institute WS COSMIC catalogue of somatic mutations in cancer. (2023). Available at: <https://cancer.sanger.ac.uk/cosmic>. (Accessed: 25th January 2024)
- Sugarbaker DJ, et al. Transcriptome sequencing of malignant pleural mesothelioma tumors. *Proc Natl Acad Sci U S A*. 2008;105:3521–6.
- Vezzani B, et al. Epigenetic regulation: a link between inflammation and carcinogenesis. *Cancers (Basel)*. 2022;14(5):1221.
- Lakshminarasimhan R, Liang G. The role of DNA methylation in cancer. *Adv Exp Med Biol*. 2016;945:151–72.
- Das PM, Singal R. DNA methylation and cancer. *J Clin Oncol*. 2004;22(22):4632–42. <https://doi.org/10.1200/JCO.2004.07.151>.
- Jones PA, Bayliss SB. The fundamental role of epigenetic events in cancer. *Nat Rev Genet*. 2002;3(3):415–28.
- Croce CM, Sozzi G, Huebner K. Role of FHIT in human cancer. *J Clin Oncol*. 1999;17(5):1618–1618. <https://doi.org/10.1200/JCO.1999.17.5.1618>.
- Tutar E, Kiyici H. Role of fragile histidine triad protein expression in pathogenesis of malignant pleural mesothelioma. *Pathology*. 2008;40:42–5.
- Pylkkänen L, et al. Reduced Fhit protein expression in human malignant mesothelioma. *Virchows Arch*. 2004;444:43–8.
- Bahari G, Hashemi M, Naderi M, Sadeghi-Bojd S, Taheri M. FHIT promoter DNA methylation and expression analysis in childhood acute lymphoblastic leukemia. *Oncol Lett*. 2017;14:5034.

35. Wu B, et al. PLXDC2 enhances invadopodium formation to promote invasion and metastasis of gastric cancer cells via interacting with PTP1B. *Clin Exp Metastasis*. 2022;39:691–710.
36. Tomasetti M, Gaetani S, Monaco F, Neuzil J, Santarelli L. Epigenetic regulation of miRNA expression in malignant mesothelioma: mirnas as biomarkers of early diagnosis and therapy. *Front Oncol*. 2019;9:1293.
37. Nicolò L, Cappellesso R, Sanavia T, Guzzardo V, Fassina A. MiR-21 over-expression and programmed cell death 4 down-regulation features malignant pleural mesothelioma. *Oncotarget*. 2018;9:17300.
38. Moore LD, Le T, Fan G. DNA methylation and its basic function. *Neuropsychopharmacol*. 2012;38:23–38.
39. Jenike AE, Halushka MK. miR-21: a non-specific biomarker of all maladies. *Biomark Res*. 2021;9:1–7.
40. Kirschner MB, et al. MiR-score: A novel 6-microRNA signature that predicts survival outcomes in patients with malignant pleural mesothelioma. *Mol Oncol*. 2015;9:715–26.
41. Wang W, et al. RNF39 mediates K48-linked ubiquitination of DDX3X and inhibits RLR-dependent antiviral immunity. *Sci Adv*. 2021. <https://doi.org/10.1126/sciadv.abe5877>.
42. Feng L, et al. Comprehensive analysis of E3 ubiquitin ligases reveals ring finger protein 223 as a novel oncogene activated by KLF4 in pancreatic cancer. *Front Cell Dev Biol*. 2021. <https://doi.org/10.3389/fcell.2021.738709>.
43. Liu J, et al. Identification of key genes and pathways associated with cholangiocarcinoma development based on weighted gene correlation network analysis. *PeerJ*. 2019;2019: e7968.
44. Bauer MA, et al. Genome-wide dna methylation signatures predict the early asymptomatic doxorubicin-induced cardiotoxicity in breast cancer. *Cancers (Basel)*. 2021;13:6291.
45. Li YD, et al. Pan-cancer analysis identifies SPEN mutation as a predictive biomarker with the efficacy of immunotherapy. *BMC Cancer*. 2023;23:1–14.
46. Li Y, et al. SPEN induces miR-4652–3p to target HIPK2 in nasopharyngeal carcinoma. *Cell Death Dis*. 2020;117(11):1–12.
47. Légaré S, et al. The estrogen receptor cofactor SPEN functions as a tumor suppressor and candidate biomarker of drug responsiveness in hormone-dependent breast cancers. *Cancer Res*. 2015;75:4351–63.
48. Meng Y, et al. Genome-wide association analyses identify CATSPERE as a mediator of colorectal cancer susceptibility and progression. *Cancer Res*. 2022;82:986–97.
49. Weisenberger DJ, Liang G. Contributions of DNA methylation aberrancies in shaping the cancer epigenome. *Transl Cancer Res*. 2015;4:219–34.
50. Wang W, et al. SEPT9: From pan-cancer to lung squamous cell carcinoma. *BMC Cancer*. 2024;24:1–20.
51. Song L, Li Y. SEPT9: a specific circulating biomarker for colorectal cancer. *Adv Clin Chem*. 2015;72:171–204.
52. Li R, Wang X, Zhu C, Wang K. lncRNA PVT1: a novel oncogene in multiple cancers. *Cell Mol Biol Lett*. 2022;27:1–44.
53. Ehrlich M. DNA hypomethylation in cancer cells. *Epigenomics*. 2009;1:239.
54. Endo Y, et al. Genome-wide DNA hypomethylation drives a more invasive pancreatic cancer phenotype and has predictive occult distant metastasis and prognosis potential. *Int J Oncol*. 2022. <https://doi.org/10.3892/ijo.2022.5351>.
55. Romero-García S, Prado-García H, Carlos-Reyes A. Role of DNA methylation in the resistance to therapy in solid tumors. *Front Oncol*. 2020;10:1152.
56. Li J, et al. The prognostic value of global DNA hypomethylation in cancer: a meta-analysis. *PLoS One*. 2014;9:e106290.
57. Bric L, Kern I. Clinical significance of histologic subtyping of malignant pleural mesothelioma. *Transl Lung Cancer Res*. 2020;9:924.
58. Capper D, et al. DNA methylation-based classification of central nervous system tumours. *Nature*. 2018;555:469–74.
59. Goto Y, et al. Epigenetic profiles distinguish malignant pleural mesothelioma from lung adenocarcinoma. *Cancer Res*. 2009;69:9073–82.
60. Dietz S, et al. Global DNA methylation reflects spatial heterogeneity and molecular evolution of lung adenocarcinomas. *Int J Cancer*. 2019;144:1061–72.
61. Jurmeister P, et al. Machine learning analysis of DNA methylation profiles distinguishes primary lung squamous cell carcinomas from head and neck metastases. *Sci Transl Med*. 2019;11:8513.
62. Cho JW, et al. Genome-wide identification of differentially methylated promoters and enhancers associated with response to anti-PD-1 therapy in non-small cell lung cancer. *Exp Mol Med*. 2020;52:1550.
63. Cho JW, et al. The importance of enhancer methylation for epigenetic regulation of tumorigenesis in squamous lung cancer. *Exp Mol Med*. 2022;54:12.
64. Meiller C, et al. Multi-site tumor sampling highlights molecular intra-tumor heterogeneity in malignant pleural mesothelioma. *Genome Med*. 2021. <https://doi.org/10.1186/s13073-021-00931-w>.
65. Guidry K, et al. DNA methylation profiling identifies subgroups of lung adenocarcinoma with distinct immune cell composition, DNA methylation age, and clinical outcome. *Clin Cancer Res*. 2022;28:3824–35.

Publisher's Note

Springer Nature remains neutral with regard to jurisdictional claims in published maps and institutional affiliations.